

Cite this: *Mater. Adv.*, 2022,  
3, 7810Received 15th July 2022,  
Accepted 21st September 2022

DOI: 10.1039/d2ma00824f

rsc.li/materials-advances

## Nanostructured Ni(OH)<sub>2</sub>–ZnO mixed crystals as recyclable catalysts for the synthesis of *N*-unsubstituted 1,2,3-triazoles†

Priyanuj Krishnann Hazarika, Priyanka Gogoi, Roktopol Hazarika,  
Kalyanjyoti Deori \* and Diganta Sarma \*

**A novel and sustainable way of constructing medicinally active compounds, 4-aryl-1,2,3-(NH)-triazoles, has been developed by employing Ni(OH)<sub>2</sub>–ZnO nanostructured mixed crystals. The one-pot multicomponent synthesis giving nanosheet-like reusable catalysts in PEG-400 solvent is quite efficient, economical and can tolerate a wide range of substrates with excellent yields.**

Nanostructured materials have been harnessed in an array of revolutionary applications<sup>1</sup> as an alternative to traditional catalysts in a greener and more sustainable way, mainly due to their incredible surface-areas<sup>2</sup> and tremendous mechanical<sup>3</sup> and catalytic<sup>4</sup> properties. In addition, good selectivity, high stability and recyclability have manifested these materials to be involved as a potent applicant in various organic reactions such as chemo-selective oxidation,<sup>5</sup> oxidative amination,<sup>6</sup> *ipso* hydroxylation<sup>7</sup> and many more.<sup>8–10</sup>

The enormous applicability of nanomaterials has encouraged us to incorporate them into the synthesis of a biologically active heterocyclic scaffold, NH-1,2,3-triazole, using a greener approach. This five-membered aromatic nucleus belongs to the kingdom of 1,2,3-triazoles. Due to its good resemblance to the amide bonds, this structural motif has been exploited for the synthesis of a large number of medicinal scaffolds<sup>11</sup> to treat deadly diseases like AIDS, cancer and tuberculosis. In particular, 4-(2-chlorophenyl)-1*H*-1,2,3-triazole possesses some intriguing features to act as an IDO (indoleamine 2,3-dioxygenase) inhibitor for cancer immunotherapy<sup>12</sup> and 4-(3,4-dibromophenyl)-1*H*-1,2,3-triazole serves as a methionine aminopeptidase enzyme<sup>13</sup> that produces anticancer and antibacterial agents.

Various methodologies have been put forward to access these compounds that mainly follow the general procedures such as the condensation reaction between olefin and azides<sup>14</sup> or the direct reaction between sodium azide and nitroolefin<sup>15</sup>

or the multicomponent synthesis from a nitroalkane, aldehyde and NaN<sub>3</sub>.<sup>16</sup> However, a large number of these protocols mainly use copper<sup>17</sup> or palladium<sup>18</sup>-based catalysts and other catalytic systems such as Amberlyst,<sup>19</sup> *p*-TsOH,<sup>20</sup> Bi<sub>2</sub>WO<sub>6</sub>/water,<sup>21</sup> *etc.*, which limits their practical use at industrial levels including low yield or substrate polymerization.<sup>22</sup> Moreover, copper is cytotoxic to mammalian cells, which hinders the use of these protocols in biological systems.<sup>23</sup>

Thus, owing to an increasing demand for the development of a sustainable strategy for the synthesis of NH-triazole, we have pioneered a greener and an efficient catalytic system for the aforementioned purposes. As such, ZnO nanoparticles stabilized/supported on CTAB (cetyl trimethyl ammonium bromide) as a highly stable catalyst have been selected for our study. This biodegradable and non-toxic white powder material has a large energy band gap (3.37 eV) and 60 meV bonding energy, which endows it with tremendous chemical and thermal stabilities.<sup>24</sup> Moreover, ZnO NPs have a large surface area and their morphologies such as nanowires<sup>25</sup> or nanorods<sup>26</sup> can be modified by controlling the reaction time, temperature or surfactants<sup>27</sup> and this makes the nanoparticles highly effective as a heterogenous catalyst.<sup>28</sup> CTAB here acts as a stabilizer or capping agent that prevents the particles from agglomerating by obstructing overgrowth of these particles.<sup>29</sup>

However, when we explored the catalytic activity of ZnO supported on CTAB nanomaterials in the multicomponent synthesis of *N*-unsubstituted triazoles, the product obtained was not very satisfactory. In recent years, nickel-based catalysts have been in the spotlight for the development of *N*-substituted 1,2,3-triazoles.<sup>30–34</sup> Getting fortified from these works, we thought of incorporating nickel into our catalytic system with a view that it may introduce some synergistic effect on ZnO nanoparticles, which will enhance the formation of *N*-unsubstituted triazoles with a gratifying yield. Hence, by using the co-precipitation method, we prepared Ni(OH)<sub>2</sub>–ZnO nanostructured mixed crystals, which when added to the reaction mixture produced the desired triazole with an excellent yield (~96%)(Fig. S1, ESI†).

Department of Chemistry, Dibrugarh University, Dibrugarh, Assam 786004, India.  
E-mail: kalchemdu@gmail.com, dsarma22@gmail.com

† Electronic supplementary information (ESI) available: NMR, SEM and optimization tables. See DOI: <https://doi.org/10.1039/d2ma00824f>



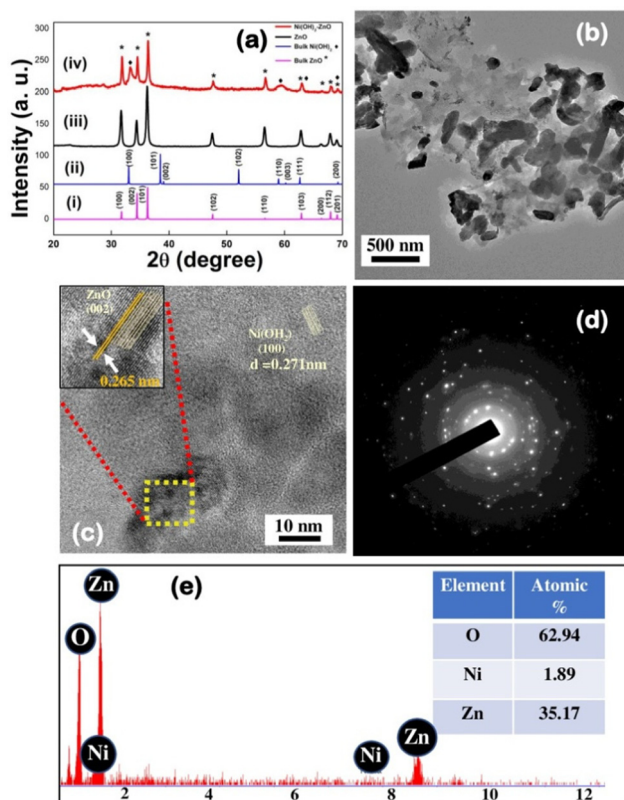


**Fig. 1** (a) The PXRD patterns of (i) bulk ZnO, (ii) bulk Ni(OH)<sub>2</sub>, (iii) as-synthesized ZnO and (iv) as-synthesized Ni-ZnO NPs. (b) The low resolution TEM micrograph. (c) The phase contrast HR-TEM image. (d) The SAED pattern and (e) SEM-EDS spectrum of the as-synthesized Ni(OH)<sub>2</sub>-ZnO nanocrystal.

The as-synthesized ZnO and Ni(OH)<sub>2</sub>-ZnO nanocrystals were probed for structural and morphology study with the help of powder XRD and HRTEM analysis. As can be seen from Fig. 1a(iii), all the distinct XRD peaks are completely matching with the wurtzite structure of ZnO (JCPDS card no. 005-0064, space group *P*<sub>6<sub>3</sub>*mc*</sub>). After addition of nickel precursor to the zinc acetate solution, the PXRD of the final crystalline precipitate exhibited two additional characteristic peaks at 33° and 60° corresponding to the (100) and (003) planes of Ni(OH)<sub>2</sub> (JCPDS card no. 14-117, space group *P*<sub>3*m*1</sub>) [Fig. 1a(iv)]. As suggested by XRD, the crystal growth of the as-synthesized nanocrystal is along the highest intensity peak, *i.e.* along the (101) plane, which justifies the sheet-like morphology of the above-mentioned nanocrystal.<sup>35</sup> The low magnification TEM image shows that the as-prepared Ni(OH)<sub>2</sub>-ZnO nanocrystals consist of sheet-like architectures of irregular shapes (Fig. 1b). Focusing on individual sheets under HRTEM clearly visualizes the lattice fringes of the (002) planes of ZnO and (100) planes of Ni(OH)<sub>2</sub>, which clearly indicates the formation of mixed crystal type nanostructured particles (Fig. 1c). The interplanar distance between the (002) planes of ZnO is measured to be 2.65 nm, which matches well with the standard data.<sup>36</sup> The selected area electron diffraction (SAED) pattern depicts the pure crystalline nature of the nanocrystal (Fig. 1d). The surface topography has

been studied with the help of field emission scanning electron microscopy (FESEM) showing hazy cloud-like morphology of the nanocrystal (Fig. S2, ESI<sup>†</sup>). EDX justifies the presence of all the elements with stoichiometric ratios in the as-synthesized nanocrystal (Fig. 1e).

To further confirm the oxidation state of the metals present in the Ni(OH)<sub>2</sub>-ZnO nanocrystal, high resolution XPS was performed. The Zn 2p spectrum in Fig. 2a depicts the presence of two doublets of binding energies of 1021.3 eV and 1044.5 eV, which can be assigned to Zn 2p<sub>3/2</sub> and Zn 2p<sub>1/2</sub>, respectively. The difference in binding energies between the two peaks is 23.2 eV which reveals the presence of ZnO in the crystal.<sup>37-39</sup> The O 1s spectrum in Ni(OH)<sub>2</sub>-ZnO (Fig. 2b) shows its standard binding energy peak at 531.3 eV. Fig. 2c shows Ni 2p<sub>3/2</sub> and Ni 2p<sub>1/2</sub> core peaks appearing at 856.2 eV and 873.8 eV with energy spacing of 17 eV. The corresponding satellite peaks are observed at 862.4 eV and 880.4 eV and have the same energy spacing of 17 eV, which indicates the presence of Ni(OH)<sub>2</sub> with Ni in 2+ oxidation state.<sup>40</sup> The survey spectrum (Fig. 2d) of the sample confirms the presence of 2p states of both Ni and Zn along with 1s states of oxygen and carbon.

The catalytic activity of the newly developed nanomaterial was studied for the synthesis of 4-aryl-NH-1,2,3-triazoles for which 4-chlorobenzaldehyde (1 mmol), nitromethane (2 mmol) and sodium azide (3 mmol) were chosen as the model substrates. The reaction was performed in PEG-400 at 100 °C and the results obtained are depicted in Table S1 (ESI<sup>†</sup>). Different quantities of the catalyst were used for investigation and it was found that with 25 mg of the catalyst, the desired product was obtained in a superior yield (96%). However, with a decrease in catalyst loading from 25 mg to 15 mg and 10 mg, the progress of the reaction was hampered and none of them exhibited better yields than the former amount (Table S1, ESI<sup>†</sup>).

In order to find the most appropriate solvent, different polar and non-polar solvents were screened and PEG-400 was found to be the best solvent. Remarkably, water and ethanol failed to

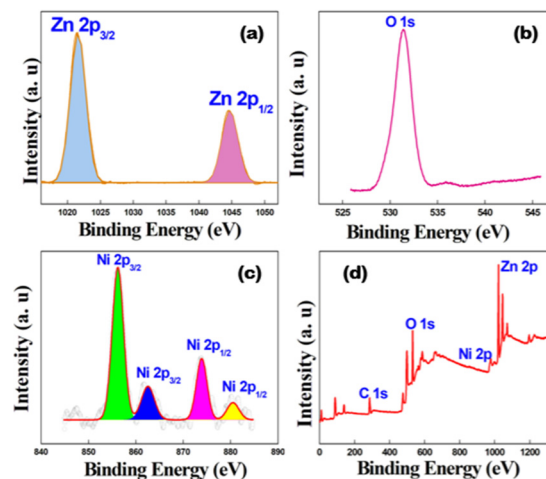


**Fig. 2** The high resolution XPS spectra of (a) Zn 2p, (b) O 1s, and (c) Ni 2p and (d) the wide survey scan of the as-synthesized Ni(OH)<sub>2</sub>-ZnO nanocrystal.



promote the reaction with better yields probably due to the low solubility of the substrates in these polar solvents. When the feasibility of this catalytic system was evaluated with different solvents such as dimethylsulphoxide (DMSO), dimethylformamide (DMF), dichloromethane (DCM), ethylene glycol and toluene, the cycloadduct was produced with relatively inferior yields (Table S2, ESI†).

When the reaction was performed at room temperature, only a trace amount of the product was obtained even after increasing the amount of the catalyst and the time duration for more than 4 hours. However, on elevating the temperature, the reaction began to show much improved yield. At 100 °C, the reaction afforded the 4-aryl-NH-1,2,3-triazoles with the best yield signifying it to be the optimum temperature (Table S2, ESI†).

Furthermore, reaction with zinc acetate and nickel acetate as the catalysts could produce the product in 45% and 50% yields, respectively. Moreover, in the absence of the catalyst, the result acquired is quite unsatisfactory, which clearly articulated the need for the developed catalyst (Table S3, ESI†).

Next, we explored various aromatic aldehydes and nitroalkanes in order to evaluate the applicability of the catalyst (Scheme 1). The reaction of benzaldehyde with nitromethane under the optimized catalytic conditions provided the corresponding triazole in 88% yield (**4f**). On exploring other aromatic aldehydes bearing various functional groups, it was found that substrates bearing halo substituents such as fluoro, bromo and chloro (**4a**, **4b**, **4d**, **4e**, **4j**, and **4m**) and nitro groups (**4c**) afforded the respective triazoles with 75–96% yield. However, 4-cyanobenzaldehyde yielded the triazole product with a lower yield (**4o**).

Aldehydes containing electron-donating groups such as hydroxyl (**4g**) or methyl (**4h**) also participated smoothly under the reaction conditions. In addition to this, heterocyclic aldehydes

also get transformed into the desired products with excellent yields (**4i**, **4k**, and **4p**). Furthermore, the reactions of nitroethane with different aldehydes were investigated and they reacted with ease to form NH-triazoles with good yields (**4n**, **4l**). From Scheme 1, it could be summarized that the newly developed catalyst is quite amicable to a wide range of aldehydes and nitroalkanes regardless of the electronic nature of the substituents present on the aldehydes and nitroalkanes.

Moreover, the catalyst can be reused successfully for up to three times without any significant drop in its activity (Fig. S3, ESI†).

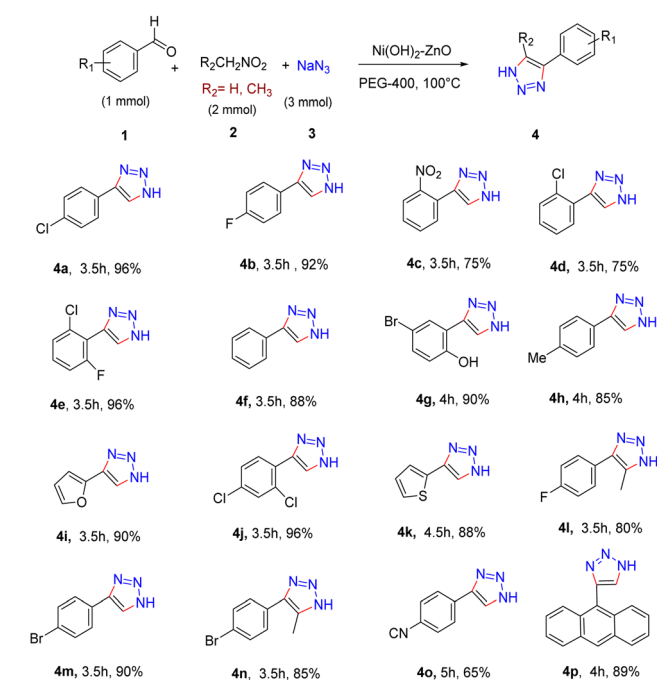
In order to demonstrate the synthetic effectiveness of this protocol on an industrial level, we performed two gram-scale reactions using 4-fluorobenzaldehyde and 4-bromobenzaldehyde and both of them yielded the respective triazoles in appreciable yields (Table S4, ESI†).

The enhanced catalytic activity of the mixed nanostructured Ni(OH)<sub>2</sub>-ZnO crystal is believed to be due to the synergistic effect of both Ni and Zn. Here, zinc oxide acts as the active site, which is attacked by the oxygen atom of the nitroolefin because zinc oxide is Lewis acidic in nature.<sup>41</sup> Ni(OH)<sub>2</sub>, on the other hand, may impose some synergistic effect on ZnO nanomaterials, which enhances the yield of the *N*-unsubstituted triazoles. The synergistic effect of Ni(OH)<sub>2</sub> and ZnO can be demonstrated from our experimental works as shown in Table S3 (ESI†). When ZnO nanomaterial was used alone for carrying out the reaction, a yield of about 80% of the NH-triazole was obtained. Similarly, Ni(OAc)<sub>2</sub> and Ni(OH)<sub>2</sub>, used alone gave only 50% and 45% yields of the desired product, respectively. But, when the catalyst Ni(OH)<sub>2</sub>-ZnO was employed for the multicomponent reaction, 96% of the product was formed, which indicates that Ni and Zn may have some cooperative effect on each other.<sup>42</sup>

Based on the literature a plausible mechanism has been proposed. The mechanism first involves the reaction between nitroalkane and aldehyde to form nitrostyrene, which coordinates with the surface of the catalyst (**A**). Then, the nucleophilic azide adds to the electrophilic C=C double bond of the intermediate followed by cyclization and loss of a nitro group to form **B**. Further aromatisation results in the formation of the triazole with regeneration of the catalyst<sup>41</sup> (Fig. 3).

Our catalytic system, Ni(OH)<sub>2</sub>-ZnO nanostructured mixed crystals, is believed to be more environmental friendly and efficient than the previous works for the synthesis of the NH-triazoles. We have compared our protocol with the literature reports (Scheme 2).<sup>15,20,43</sup>

In a nutshell, we have prepared a highly stable heterogeneous catalyst that showed appreciable catalytic activity in the multicomponent synthesis of 4-aryl-NH-1,2,3-triazoles. The Ni(OH)<sub>2</sub>-ZnO mixed nanocrystals supported on CTAB are simple to prepare, sturdy, recoverable and easily reusable for up to three times without any significant loss in their catalytic performance. Apart from this, the catalyst is also able to tolerate a wide range of aldehydes and nitroalkanes, which makes this methodology suitable for the sustainable synthesis of various unsubstituted NH-triazoles.



Scheme 1 Substrate scope.



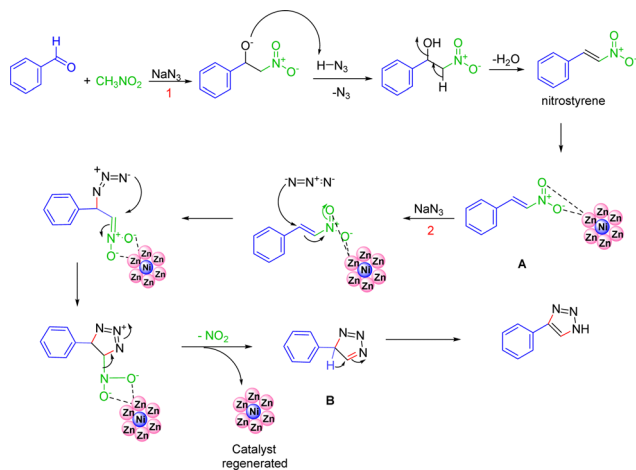
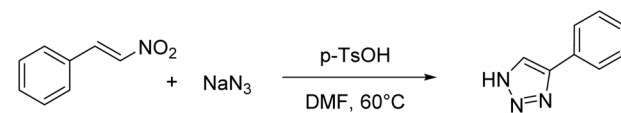
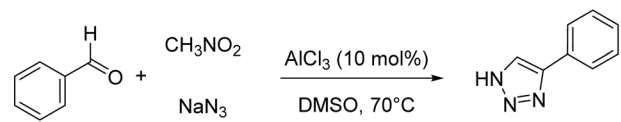
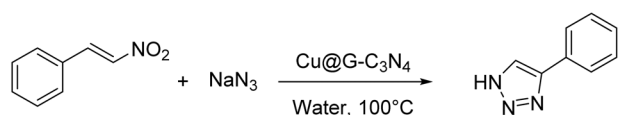
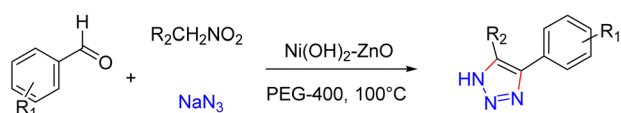


Fig. 3 Mechanistic overview of the Ni(OH)<sub>2</sub>-ZnO-catalysed 4-aryl-NH-1,2,3-triazole synthesis.

### Previous Works:



### Our Work:



Scheme 2 Comparison of the developed protocol with the literature reports.

## Conflicts of interest

There are no conflicts to declare.

## Acknowledgements

D. S. and K. D. are thankful to CSIR, New Delhi, India for a research grant [Grant No. 02(0399)/21/EMR-II]. K. D. is grateful to SERB-DST, India (Grant EEQ/2018/000326) for financial assistance. P. K. H. thanks CSIR, New Delhi for a research fellowship. The authors acknowledge IISER-Mohali for TEM analysis, CSIR-NEIST Jorhat for XPS, STIC Cochin for XRD,

CSIC Dibrugarh University for NMR measurements and Dibrugarh University for providing all infrastructural facilities.

## Notes and references

- (a) H. B. Dias, M. I. B. Bernardi, V. S. Marangoni, A. C. de, A. Bernardi, A. N. S. Rastelli and A. C. Hernandez, *Mater. Sci. Eng., C*, 2019, **96**, 391; (b) M. B. Gawande, P. S. Branco and R. S. Varma, *Chem. Soc. Rev.*, 2013, **42**, 3371; (c) D. Astruc, F. Lu and J. R. Aranzas, *Angew. Chem., Int. Ed.*, 2005, **44**, 7852; (d) R. S. Varma, *Green Chem.*, 2014, **16**, 2027; (e) J. Damodharan, *Mater. Today*, 2021, **37**, 383.
- J. Govan and Y. K. Gun'ko, *Nanomaterials*, 2014, **4**, 222.
- D. Guo, G. Xie and J. Luo, *J. Phys. D: Appl. Phys.*, 2014, **47**, 013001.
- M. C. Daniel and D. Astru, *Chem. Rev.*, 2004, **104**, 293.
- A. Saxena, A. Kumar and S. Mozumdar, *J. Mol. Catal. A: Chem.*, 2007, **269**, 35.
- M. Behzadi, M. M. Hashemi, M. Rognizadeh, S. Nasiri and A. R. Saadatabadi, *New J. Chem.*, 2021, **45**, 3242.
- V. Sadhasivam, M. Harikrishnan, G. Elamathi, R. Balasaravanan, S. Murugesan and A. Siva, *New J. Chem.*, 2020, **44**, 6222.
- L. L. Chng, N. Erathodiyil and J. Y. Ying, *Acc. Chem. Res.*, 2013, **46**, 1825.
- K. Hong, M. Sajjadi, J. M. Suh, K. Zhang, M. Nasrollahzadeh, H. W. Jang, R. S. Varma and M. Shokouhimehr, *ACS Appl. Nano Mater.*, 2020, **3**, 2070.
- A. M. Ferretti, A. Ponti and G. Molteni, *Tetrahedron Lett.*, 2015, **56**, 5727.
- (a) L. S. Kallander, Q. Lu, W. Chen, T. Tomaszek, G. Yang, D. Tew, T. D. Meek, G. A. Hofmann, C. K. Schulz-Pritchard, W. W. Smith, C. A. Janson, M. D. Ryan, G. F. Zhang, K. O. Johanson, R. B. Kirkpatrick, T. F. Ho, P. W. Fisher, M. R. Mattern, R. K. Johnson, M. J. Hansbury, J. D. Winkler, K. W. Ward, D. F. Veber and S. K. Thompson, *J. Med. Chem.*, 2005, **48**, 5644; (b) T. Weide, S. A. Saldanha, D. Minond, T. P. Spicer, J. R. Fotsing, M. Spaargaren, J.-M. Frère, C. Bebrone, K. B. Sharpless, P. S. Hodder and V. V. Fokin, *ACS Med. Chem. Lett.*, 2010, **1**, 150; (c) A. R. Gakovic, J. J. Csanádi, E. A. Djurendic, O. Klisuric, G. Bogdanovic and K. M. P. Gaši, *Tetrahedron Lett.*, 2009, **50**, 4107; (d) Q. Huang, M. Zheng, S. Yang, C. Kuang, C. Yu and Q. Yang, *Eur. J. Med. Chem.*, 2011, **46**, 5680; (e) U. F. Röhrig, S. R. Majjigapu, A. Grosdidier, S. Bron, V. Stroobant, L. Pilotte, D. Colau, P. Vogel, B. J. Van den Eynde, V. Zoete and O. Michielin, *J. Med. Chem.*, 2012, **55**, 5270.
- U. F. Röhrig, L. Awad, A. Grosdidier, P. Larrieu, V. Stroobant, D. Colau, V. Cerundolo, A. J. G. Simpson, P. Vogel and B. Van den Eynde, *J. Med. Chem.*, 2010, **53**, 1172.
- L. S. Kallander, Q. Lu, W. Chen, T. Tomaszek, G. Yang, D. Tew, T. D. Meek, G. A. Hofmann, C. K. Schulz-Pritchard and W. W. Smith, *J. Med. Chem.*, 2005, **48**, 5644.
- (a) J. Li, D. Wang, Y. Zhang, J. Li and B. Chen, *Org. Lett.*, 2009, **11**, 3024; (b) T. Jin, S. Kamijo and Y. Yamamoto, *Tetrahedron Lett.*, 2004, **45**, 9435; (c) L. H. Lu, J. H. Wu and C. H. Yang, *J. Chin. Chem. Soc.*, 2008, **55**, 414.





- 15 S. Payra, A. Saha and S. Banerjee, *ChemCatChem*, 2018, **10**, 5468.
- 16 A. Garg, R. Hazarika, N. Dutta, B. Dutta and D. Sarma, *ChemistrySelect*, 2021, **6**, 7266.
- 17 Y. Chen, G. Nie, Q. Zhang, S. Ma, H. Li and Q. Hu, *Org. Lett.*, 2015, **17**, 1118.
- 18 J. John, J. Thomas, N. Parekh and W. Dehaen, *Eur. J. Org. Chem.*, 2015, 4922.
- 19 H. Zhang, D. Z. Dong and Z. L. Wang, *Synthesis*, 2016, 131.
- 20 X. J. Quan, Z. H. Ren, Y. Y. Wang and Z. H. Guan, *Org. Lett.*, 2014, **16**, 5728.
- 21 B. Paplal, S. Nagaraju, V. Palakollu, S. Kanvah, B. V. Kumar and D. Kashinath, *RSC Adv.*, 2015, **5**, 57842.
- 22 A. Saha, C. M. Wu, R. Peng, R. Koodali and S. Banerjee, *Eur. J. Org. Chem.*, 2019, 104.
- 23 (a) A. J. Link, M. K. S. Vink, N. J. Agard, J. A. Prescher, C. R. Bertozzi and D. A. Tirrell, *Proc. Natl. Acad. Sci. U. S. A.*, 2006, **103**, 10180; (b) G. J. Brewer, *Chem. Res. Toxicol.*, 2010, **23**, 319.
- 24 (a) D. C. Kennedy, C. S. McKay, M. C. B. Legault, D. C. Danielson, J. A. Blake, A. F. Pegoraro, A. Stolow, Z. Mester and J. P. Pezacki, *J. Am. Chem. Soc.*, 2011, **133**, 17993; (b) M. Aminuzzaman, L. P. Ying, W.-S. Goh and A. Watanabe, *Bull. Mater. Sci.*, 2018, **41**, 1.
- 25 V. Errico, G. Arrabito, E. Fornetti, C. Fuoco, S. Testa, G. Saggio, S. Rufini, S. Cannata, A. Desideri and C. Falconi, *ACS Appl. Mater. Interfaces*, 2018, **10**, 14097.
- 26 P. Ravirajan, A. M. Peiró, M. K. Nazeeruddin, M. Graetzel, D. D. C. Bradley, J. R. Durrant and J. Nelson, *J. Phys. Chem. B*, 2006, **110**, 7635.
- 27 A. Sirelkhatim, S. Mahmud, A. Seeni, N. H. M. Kaus, L. C. Ann, S. K. M. Bakhori, H. Hasan and D. Mohamad, *Nano-Micro Lett.*, 2015, **7**, 219.
- 28 J. Strunk, K. Kahler, X. Xia and M. Muhler, *Surf. Sci.*, 2009, **603**, 1776.
- 29 (a) J. Tang, J. Huang and S. Q. Man, *Spectrochim. Acta, Part A*, 2013, **103**, 349; (b) P. Phukan, S. Agarwal, K. Deori and D. Sarma, *Catal. Lett.*, 2020, **150**, 2208.
- 30 S. Boggala, V. Perupogu, S. Varimalla, K. Manda and V. Akula, *Mol. Catal.*, 2022, **521**, 112191.
- 31 V. Camberlein, N. Kraupner, N. B. Karroum, E. Lipka, R. D. Poulain, B. Deprez and D. Bosc, *Tetrahedron Lett.*, 2021, **73**, 153131.
- 32 W. G. Kim, M. E. Kang, J. B. Lee, M. H. Jeon, S. Lee, J. Lee, B. Choi, P. M. S. D. Cal, S. Kang, J. M. Kee, G. J. L. Bernardes, J. U. Rohde, W. Choe and S. Y. Hong, *J. Am. Chem. Soc.*, 2017, **139**, 12121.
- 33 Z. Hashemi, J. Albadi and M. Jalal, *Res. Chem. Intermed.*, 2021, **47**, 5291.
- 34 P. Choudhury, S. Chattopadhyay, G. De and B. Basu, *Mater. Adv.*, 2021, **2**, 3042.
- 35 Q. Wang, D. Yang, Y. Qiu, X. Zhang, W. Song and Lizhong Hu, *Appl. Phys. Lett.*, 2018, **112**, 063906.
- 36 X. Li, Y. Li, G. Sun, N. Luo, B. Zhang and Z. Zhang, *Nanomaterials*, 2019, **9**, 723.
- 37 S. S. Patil, M. G. Mali, M. S. Tamboli, D. R. Patil, M. V. Kulkarni, H. Yoon, H. Kim, S. S. Al-Deyab, S. S. Yoon, S. S. Kolekar and B. B. Kale, *Catal. Today*, 2016, **260**, 126.
- 38 J. Das, S. K. Pradhan, D. R. Sahu, D. K. Mishra, S. N. Sarangi, B. B. Nayak, S. Verma and B. K. Roul, *J. Appl. Phys.*, 2011, **109**, 103508.
- 39 R. Gaashani, S. Radiman, A. R. Daud, N. Tabet and Y. Al-Douri, *Ceram. Int.*, 2013, **39**, 2283.
- 40 M. Kumar and S. Deka, *ACS Appl. Mater. Interfaces*, 2014, **6**, 16071.
- 41 R. Hazarika, A. Garg, S. Chetia, P. Phukan, A. Kulshrestha, A. Kumar, A. Bordoloi, A. J. Kalita, A. K. Guha and D. Sarma, *Appl. Catal., A*, 2021, **625**, 118338.
- 42 H. Inagaki, A. Nishikawa, Y. Sugita and T. Tsuji, *J. Nucl. Sci. Technol.*, 2003, **3**, 143.
- 43 Q. Hu, Y. Liu, X. Deng, Y. Li and Y. Chena, *Adv. Synth. Catal.*, 2016, 358.

